Published in final edited form as:
Neuroscience. 2014 February 14; 259: 94–100. doi:10.1016/j.neuroscience.2013.11.052.

Treatment Effects in a Transgenic Mouse Model of Alzheimer's Disease: A Magnetic Resonance Spectroscopy Study after Passive Immunization

Małgorzata Marjańska, PhD[1], **Stephen D. Weigand, MS**[2], **Gregory Preboske, MS**[3], **Thomas M. Wengenack, PhD**[4], **Ryan Chamberlain, PhD**[1], **Geoffry L. Curran, BS, BA, MBA**[4], **Joseph F. Poduslo, PhD**[4], **Michael Garwood, PhD**[1], **Dione Kobayashi, PhD**[5], **John C. Lin, MD, PhD**[5], and **Clifford R. Jack Jr., MD**[3]

[1]Center for Magnetic Resonance Research and Department of Radiology, University of Minnesota, 2021 6th ST SE, Minneapolis, Minnesota 55455, USA

[2]Department of Health Sciences Research, Mayo Clinic, Rochester, Minnesota 55902, USA

[3]Department of Radiology, Mayo Clinic College of Medicine, Rochester, Minnesota 55902, USA

[4]Departments of Neurology, Neuroscience, and Biochemistry/Molecular Biology, Mayo Clinic College of Medicine, Rochester, Minnesota 55902, USA

[5]Rinat, Pfizer Inc., South San Francisco, California 94080, USA

Abstract

Despite the enormous public health impact of Alzheimer's disease (AD), no disease modifying treatment has yet been proven to be efficacious in humans. A rate-limiting step in the discovery of potential therapies for humans is the absence of efficient non-invasive methods of evaluating drugs in animal models of disease. Magnetic resonance spectroscopy (MRS) provides noninvasive way to evaluate the animals at baseline, at the end of treatment, and serially to better understand treatment effects. In this study, MRS was assessed as potential outcome measure for detecting disease modification in a transgenic mouse model of AD. Passive immunization with two different antibodies, which have been previously shown to reduce plaque accumulation in transgenic AD mice, was used as intervention. Treatment effects were detected by MRS, and the most striking finding was attenuation of *myo*-inositol increases in APP-PS1 mice with both treatments. Additionally, a dose dependent effect was observed with one of the treatments for *myo*-inositol. MRS appears to be a valid *in vivo* measure of anti-Aβ therapeutic efficacy in pre-clinical studies. Because it is noninvasive, and can detect treatment effects, use of MRS-based endpoints could substantially accelerate drug discovery.

Keywords

MRS; treatment detection; *myo*-inositol; *N*-acetylaspartate

Corresponding author and reprint info: Małgorzata Marjańska, PhD Center for Magnetic Resonance Research 2021 6th Street SE Minneapolis, MN 55455 United States Phone: 1-612-626-2001 Fax: 1-612-626-2004 gosia@cmrr.umn.edu.

The authors, except for Dione Kobayashi and John C. Lin, declare no competing financial interest.

1. Introduction

Alzheimer's disease (AD) is the most common cause of dementia in elderly (Hebert et al., 2003). The vast majority of cases are sporadic with symptom onset typically after age 65. A small percentage of cases are familial with much younger onset. While quite uncommon, genetically determined AD has provided invaluable insight into the etiology of the disease. AD cases that are attributed to specific mutations involve one of three genes that alter production, aggregation or clearance of β–amyloid protein (Selkoe, 1995, 1998). Murine models of brain β–amyloidosis have been created by inserting one or more of these human mutations into the mouse genome (Hsiao et al., 1996, Holcomb et al., 1998). These transgenic mice display extensive amyloid plaque formation and enable controlled study of disease mechanisms and testing of anti-amyloid interventions.

^{1}H magnetic resonance spectroscopy (MRS) has been shown to be sensitive to age-dependent metabolite changes in APP-PS1 mice which differ dramatically from the metabolic profile of age-matched wild-type mice (Marjanska et al., 2005).

Peripheral administration of anti-Aβ antibodies to AD transgenic mice, so-called passive immunization, can significantly reduce amyloid plaque burden and improve memory performance in these mice (Bard et al., 2000, DeMattos et al., 2001, Wilcock et al., 2004a, Wilcock et al., 2004b, Hartman et al., 2005). Passive immunization involves injection of antibodies already raised against Aβ that bind to Aβ in circulation or to amyloid plaques in the same manner as endogenously generated antibodies.

Despite the enormous public health impact of AD, no disease modifying treatment has been approved for use in humans. A major rate-limiting step in discovery of potential disease modifying therapies for humans is the absence of efficient, longitudinal and non-invasive methods of evaluating drugs in animal models. MRS, due to its non-invasive nature, enables the assessment of animals at baseline and at the end of treatment, as well as serially throughout treatment. Each animal effectively serves as its own control and consequently increases the power and precision of estimates.

The objective of the study was to use interventions that had already been proven to reduce plaque accumulation in transgenic mice (Wilcock et al., 2006, La Porte et al., 2012) to evaluate MRS as outcome measure for detecting disease modification. The intervention employed was passive immunization with two different antibodies. Natural history studies of MRS changes in transgenic mouse models of AD with a variety of mutations have been published before (Dedeoglu et al., 2004, Marjanska et al., 2005, von Kienlin et al., 2005, Choi et al., 2007, Oberg et al., 2008, Chen et al., 2009, Chen et al., 2012, Mlynarik et al., 2012, Forster et al., 2013, Jansen et al., 2013, van Duijn et al., 2013). In addition, donepezil (Westman et al., 2009) and anti-inflammatory (Choi et al., 2010) treatments have been evaluated with MRS. In this study, we report for the first time MRS findings after immunotherapy.

2. Experimental Procedures

2.1 Animals

Double-transgenic APP-PS1 mice were cross-bred in-house. Hemizygous transgenic mice (mouse strain: C57B6/SJL; ID no. Tg2576) expressing mutant human APP_{695} containing a double mutation (K670N, M671L) (Hsiao et al., 1996) were mated with a strain of homozygous transgenic mice (mouse strain, Swiss Webster/B6D2; ID no. M146L6.2) expressing mutant human PS1 containing a single mutation (M146L) (Holcomb et al., 1998).

2.2 Intervention

Ponezumab (PF-04360365) is a humanized IgG2Δa monoclonal antibody for the treatment of AD. Ponezumab binds to the C-terminus and specifically recognizes amino acids 30-40 of the Aβ1-40 peptide. It has been hypothesized that ponezumab sequesters Aβ in the blood and shifts the brain-blood equilibrium towards the blood, depleting brain Aβ stores (Freeman et al., 2012, La Porte et al., 2012). Previous studies have demonstrated that administration of ponezumab to transgenic mice led to a dose-dependent reduction in hippocampal amyloid load (La Porte et al., 2012).

The compound, 2H6-D, a murine version of ponezumab, is a deglycosylated mouse monoclonal antibody which binds to the C-terminus of $A\beta_{1\text{-}40}$. This antibody has been shown to reduce amyloid deposition and eliminate cognitive deficits with considerable reduction in some potentially adverse vascular changes, such as CAA and microhemorrhage in transgenic mice (Wilcock et al., 2006, Karlnoski et al., 2008).

2.3 Treatment design

Sixty four APP-PS1 mice were pseudo-randomly assigned to one of the following four treatment groups: 1 mg/kg ponezumab, 3 mg/kg ponezumab, 10 mg/kg ponezumab, and 10 mg/kg control antibody so that each treatment arm was equally represented within each litter. An additional sixteen APP-PS1 mice were treated with 10 mg/kg of 2H6-D anti-Aβ monoclonal antibodies. Sixteen B6SJL wild-type (WT) mice were treated with 10 mg/kg of PBS negative control on the same schedule as the treated animals. Treatment was started at 12 months of age, lasted for 4 months, and consisted of weekly intra-peritoneal injections of the antibodies supplied by Pfizer, Inc.

2.4 Animal preparation for MR experiments

Experimental protocols were approved by the Institutional Animal Care and Use Committees in accordance with the National Institutes of Health *Guide for the Care and Use of Laboratory Animals*. Mice were anesthetized by using 1.0-1.5% isoflurane and O_2/N_2O and positioned in custom-built device to immobilize the head during experiments. Body temperature was maintained at 37°C by warm water circulation, and physiological monitoring was used for temperature, respiration, and EEG (Jack et al., 2004).

2.5 Magnetic Resonance

Transgenic and wild-type mice at 12 months of age (before the beginning of treatment) and 16 months of age (after 4 months of treatment) were scanned *in vivo* using a 9.4-T, 31-cm horizontal bore magnet (Magnex Scientific, Oxford, UK) interfaced with a Varian INOVA console. The magnet was equipped with a gradient insert capable of reaching 30 mT/m in 300 μs (Resonance Research, Inc., Billerica, MA). A quadrature 400-MHz ^{1}H surface radiofrequency coil (two loops, 10-mm diameter) was used to transmit and receive.

In vivo ^{1}H MR spectra were acquired from an 8.7-μL volume of interest (voxel) placed in the hippocampus, somatosensory cortex, and thalamus (Fig. 1a) using localized T_2-weighted multislice rapid acquisition with relaxation enhancement (RARE) images (Hennig et al., 1986). Linewidths around 20 Hz for water were obtained after adjusting the first- and second-order shims by using FAST(EST)MAP (Gruetter, 1993, Gruetter and Tkac, 2000). Spectra were acquired with localization by adiabatic selective refocusing (LASER) (Garwood and DelaBarre, 2001). Following water suppression performed with variable pulse power and optimized relaxation delays (VAPOR) (Tkac et al., 1999), all resonances were excited using a nonselective numerically optimized adiabatic half-passage (AHP) pulse (Garwood and Ke, 1991). 3D localization was then performed with a pair of AFP pulses in

each dimension. The AHP pulse duration was 4 ms, and each AFP pulse was an offset-independent adiabatic pulse, HS1, with pulse length T_p of 1.5 ms and bandwidth of 16.7 kHz (Silver et al., 1984, Garwood and DelaBarre, 2001). The echo time (T_E) was 27 ms, and the repetition time (T_R) was 4 s. Each free induction decay (FID) was acquired with 4096 complex points using a spectral width of 10 kHz. FIDs were stored separately in the memory, and both frequency and phase were corrected based on the total creatine (tCr = creatine and phosphocreatine) signal at 3.03 ppm prior to summation. Small residual eddy current effects were corrected using a reference water signal. The spectra used in fitting were a sum of 384 scans obtained in 25 minutes.

The acquired spectra were analyzed using LCModel 6.1-4A (Provencher, 1993, 2001) (Stephen Provencher, Inc., Oakville, Ontario, Canada). The basis set for LCModel was generated using programs written in-house based on the density matrix formalism (Henry et al., 2006) in Matlab (The MathWorks, Inc., Natick, MA, USA) using the known chemical shifts and *J*-couplings (Govindaraju et al., 2000). The experimentally observed spectrum of macromolecules (Pfeuffer et al., 1999) and the simulated spectra of the following eighteen metabolites were included in the basis set for LCModel: alanine (Ala), aspartate (Asp), creatine (Cr), γ-aminobutyric acid (GABA), glucose (Glc), glutamate (Glu), glutamine (Gln), glutathione (GSH), glycerophosphorylcholine (GPC), phosphorylcholine (PCho), *myo*-inositol (mIns), lactate (Lac), *N*-acetylaspartate (NAA), *N*-acetylaspartylglutamate (NAAG), phosphocreatine (PCr), phosphorylethanolamine (PE), *scyllo*-inositol (sIns), and taurine. No baseline correction, zero-filling or line broadening were applied to the *in vivo* data prior to the analysis. The LCModel fitting was performed over the spectral range from 1.0 to 4.4 ppm. Quantification was obtained using tCr (assumed to be 8 mM) as an internal standard.

The coefficients of variation for mIns and NAA were 0.07 and 0.05, respectively. mIns was quantified with Cramér-Rao Lower Bounds (CRLBs) of 4.0 ± 0.8% and NAA with CRLBs of 2.6 ± 0.6% in all groups for both scanning sessions.

2.6 Data exclusion criteria

The treatment study was started with 80 APP-PS1 transgenic mice and 16 WT mice. Data from 31 APP-PS1 and 6 WT mice were excluded from the analyses for this study, for the following reasons: (a) 14 mice died during the treatment and did not undergo the second MRI and MRS scan; (b) 10 mice did not have plaques on Thio-S, (c) in 12 mice anti-drug antibodies were detected, and (d) in 1 control antibody mouse anti-drug antibodies were detected using antibody immunoassay in mouse plasma. At the end, data from 59 mice were used for statistical analysis with 8 mice in 1 mg/kg ponezumab, 11 mice in 3 mg/kg ponezumab, 7 mice in 10 mg/kg ponezumab, 12 mice in 2H6-D, 11 mice in control antibody, and 10 mice in WT groups.

2.7 Biochemical analysis of brain Aβ concentration

Hemibrain tissues were homogenized in 5 M guanidine HCl, and the total Aβ1-x, Aβx-40, or Aβx-42 concentrations were measured from the tissue homogenates as previously described (La Porte et al., 2012).

2.8 Statistical analysis

Differences in Aβx-40 by group were assessed using pairwise nonparametric Wilcoxon rank-sum/Mann-Whitney U tests due to strong departures from normality in this measure. Analysis of MRS data were performed using ANCOVA models in which the four-month follow-up value was the response/dependent variable, treatment group was the primary factor, and the baseline value was an adjustment covariate. This method accounts for

differences in groups at baseline and is generally preferred to analyzing change scores, defined as the follow-up value minus the baseline value, in an ANOVA model (Bonate, 2000, Senn, 2006). A trend test was performed to evaluate a dose-response effect of ponezumab by creating a numeric variable coded 0 for control, 1 for 1 mg/kg, 2 for 3 mg/kg, and 3 for 10 mg/kg with indicator variables for the 2H6-D and WT groups. Residual plots were examined to evaluate the ANCOVA assumptions of conditional normality and constant variance across groups; these assumptions were found to be reasonable and approximately satisfied. Mice not surviving to the four-month time period were treated as missing completely at random and omitted from the analyses (Little and Rubin, 2002).

Pairwise group comparisons using contrasts from the ANCOVA models were performed. Unadjusted *p*-values from these comparisons are reported but *p*-values to several significant digits are provided to allow the reader to perform adjustments as desired (O'Brien, 1983). In the context of the current study, maintaining statistical power rather than strongly controlling the false positive rate is considered important.

To graphically summarize group-wise differences in ANCOVA models, box plots of partial residuals from the model are used (Fox, 2008). These partial residual plots show the marginal effect of treatment after accounting for baseline differences. If *a* is the regression model intercept and *b* is the regression coefficient for the baseline value from the ANCOVA model, the partial residuals are defined as the follow-up value minus *a* minus *b* times the baseline value; by convention these results are centered to have mean zero. For simplicity, the *y*-axes in these plots are labeled as the baseline-adjusted four-month value.

We assessed the associations between MRS and Aβx-40 measures using Spearman's rank correlation which does not assume normal distributions or linear relationships. All statistical analyses were performed using R software version 2.13.2 (R Foundation for Statistical Computing, Vienna; http://www.r-project.org).

3. Results

3.1 Association between treatment and brain Aβx-40 levels at 4 months

Brain Aβx-40 levels by treatment group are summarized in Fig. 2. The 2H6-D group had reduced brain Aβx-40 levels relative to all groups ($p < 0.001$). Additionally, 1 mg/kg ($p = 0.02$), 3 mg/kg ($p = 0.001$), 10 mg/kg ($p = 0.02$) ponezumab groups had lower brain Aβx-40 levels than the control group.

3.2 Spectroscopy versus treatment group

The spectra shown in Fig. 1b are representative of the quality consistently achieved in this study. These spectra were analyzed with LCModel to obtain ratios of concentrations of the 16 metabolites with respect to tCr. Similar linewidths of tCr (18.6 ± 4.4 Hz) were obtained in all groups for both scanning sessions. Only changes in concentrations of mIns and NAA were observed during the treatment. There was no change observed for other metabolites.

mIns—Fig. 3a shows box plots summarizing the baseline-adjusted 4 month values for mIns/tCr by group with pairwise *p*-values from ANCOVA model contrasts summarized in panel b. There are three main findings: (a) an increase in mIns over time in vehicle treated APP-PS1 mice compared to WT mice ($p = 0.004$); (b) compared with untreated APP-PS1 mice, evidence of a dose-dependent response for ponezumab ($p = 0.02$); (c) the smallest increase in mIns in APPPS1 mice is seen with 10 mg/kg ponezumab ($p = 0.04$) and a similar difference was observed in the 2H6-D group relative to control ($p = 0.08$) with no difference between 10 mg/kg ponezumab and 2H6-D groups.

NAA—Fig. 3c shows box plots summarizing the baseline-adjusted 4 month value for NAA/tCr by group with differences summarized in panel d. There was some evidence that NAA in the 2H6-D treated mice declined less compared to 1 mg/kg ponezumab ($p = 0.08$) and 3 mg/kg ponezumab ($p = 0.03$). The WT group appeared to decline somewhat less than the 3 mg/kg ponezumab group ($p = 0.06$).

To evaluate whether MRS is sensitive to amyloid levels in APP-PS1 mice, the correlation between MRS and Aβx-40 were assessed. The correlation was +0.48 for mIns ($p = 0.001$) and -0.48 for NAA ($p < 0.001$).

4. Discussion

The major findings in this study were as follows: (a) evidence consistent with a treatment effect in brain Aβx-40 levels for ponezumab and 2H6-D; (b) both ponezumab and 2H6-D appeared to slow the rate at which mIns normally increases in APP-PS1 mice; (c) for ponezumab, the slowing of the rate of mIns increase was dose dependent.

The purpose of this study was to test the hypothesis that MRS could detect a treatment effect in APP-PS1 mice. Two treatments were evaluated that had already been shown to reduce accumulation in plaque load in transgenic mice. While treatment efficacy was verified by measuring Aβ immunochemistry (Wilcock et al., 2006) and Aβ levels in guanidine homogenates (La Porte et al., 2012), comparison of two treatments was not under investigation here. The two antibodies which were used are murine and humanized version of the same antibody which binds to the C-terminus of $A\beta_{1\text{-}40}$. Previously, the 2H6-D antibody was successful in reducing the plaque load in the cortex and hippocampus after 3 or 4 months of treatment in 19 or 20 month-old Tg2576 transgenic mice with similar doses as were used in this study (Wilcock et al., 2006, Karlnoski et al., 2008). In a prior study of ponezumab, while there were no significant decreases in cortical Aβ levels, the hippocampus showed evidence of a highly significant and dose-dependent treatment effect in 5.5 month-old APP-PS1 transgenic mice treated once with similar doses as were used in this study (La Porte et al., 2012). Based on those studies, we used 12 month old APP-PS1 mice with 4 month long treatment as in this particular mouse model plaques develop at an earlier age than in APP mice and mIns allows the differentiation between APP-PS1 and wild-type mice at this age (Marjanska et al., 2005). MRS data were obtained from a voxel placed primarily in the hippocampus and cortex (with some inclusion of thalamus) since previous therapeutic studies showed the most significant changes in plaque load in the hippocampus.

As anticipated, after 4 months of treatment, the data indicated reduced brain Aβx-40 levels in ponezumab and 2H6-D treated mice relative to control mice.

mIns increases with age in untreated AD mice. This is a dramatic effect in APP-PS1 mice, with exponential increases observed from the age of 12 months through 31 months (Marjanska et al., 2005). Indeed, this is what was seen in the untreated APP-PS1 mice in the current study. We attribute this to an association between plaque load and mIns. mIns is considered to be a marker of glial proliferation (Brand et al., 1993). Plaques are surrounded by a halo of reactive astrocytes and also have micro glia surrounding and within the plaques.

The most striking result in this study was the reduction in the rate of mIns in 2H6-D treated mice. We found the same phenomenon in a dose dependent relationship in ponezumab treated mice. The 10 mg/kg treated ponezumab mice had baseline adjusted 4 month mIns levels similar to the 2H6-D treated mice, while the 1 mg/kg ponezumab treated mice had levels similar to the vehicle control APP-PS1 mice. The fact that we found a treatment effect with 2 different (albeit closely related) antibodies, and that a dose dependent response was

seen for ponezumab, lends credibility to the conclusion that the mIns results reflect a true drug effect. Another piece of evidence supporting the conclusion that mIns is measuring a drug effect was that the concentrations of mIns at four months correlated moderately well with Aβx-40 (Spearman rank correlation, + 0.48, $p = 0.001$). Although MRS voxel included hippocampus, cortex and thalamus, the pathology is expressed equally in hippocampus and cortex (Jack et al., 2007). In humans, MRS metabolite ratios of mIns/tCr are associated with amyloid load as measured with PIB (Kantarci et al., 2011), and decrease in NAA/tCr is associated with autopsy early-stage tau pathology and neuronal loss, and elevation in mIns/tCr is associated with autopsy plaque load (Murray et al., 2013). Based on these MRS-autopsy correlations in humans, we extrapolate our mIns findings in mice to indicate a specific therapeutic effect related to amyloid plaques.

NAA is a marker of neuronal integrity. It normally declines with age in APP-PS1 mice although not nearly as dramatically as mIns increases (Marjanska et al., 2005). The NAA results suggested some evidence of neuro-protection afforded by 2H6-D as NAA levels by 4 months appeared greater than the low- and medium-dose ponezumab groups. It is likely that NAA is a less sensitive marker than mIns to the phenotype expressed by APP-PS1 mice. APP-PS1 mice are an excellent model of beta amyloidopathy. APP-PS1 mice do not, however, fully recapitulate human AD in that they do not develop neuritic plaques with tau positive neurites and do not develop notable neurodegenerative changes. Thus pathological phenotype that APP-PS1 mice display is not particularly well matched to the properties that NAA is sensitive to, i.e., neurodegeneration. Mouse models of AD provide guidance, but translating preclinical findings directly to human AD has limitations.

In conclusion, ^{1}H MRS was shown to be a valid *in vivo* measure of anti-Aβ therapeutic efficacy in pre-clinical studies. This method can be used to speed drug discovery. Accelerated throughput rates would lower costs for drug discovery and in turn translate into a greater number of compounds that can be effectively tested.

Acknowledgments

Dione Kobayashi and John C. Lin are employees of Rinat, Pfizer Inc. This work was supported by Pfizer-Rinat, NIH grants: BTRC P41 RR008079, P41 EB015894, P30 NS057091, RO1 AG11378, and the W.M. Keck Foundation. The authors would like to thank James Kupiec and Jaume Pons for helpful discussions and for initiating research support; Dawn M. Gregor for mouse breeding and genotypic; Angela L. Styczynski Snyder, Nathaniel J. Powell and Angela Polk for data acquisition; Christine O'Brien for animal care; Karin Wallace and Kelly Bales for brain homogenate assay support; Danielle Pappas for plasma drug level assays.

References

Bard F, Cannon C, Barbour R, Burke RL, Games D, Grajeda H, Guido T, Hu K, Huang J, Johnson-Wood K, Khan K, Kholodenko D, Lee M, Liebergurg I, Motter R, Nguyen M, Soriano F, Vasquez N, Weiss K, Welch B, Seubert P, Schenk D, Yednock T. Peripherally administered antibodies against amyloid beta-peptide enter the central nervous system and reduce pathology in a mouse model of Alzheimer disease. Nature Med. 2000; 6:916–919. [PubMed: 10932230]

Bonate, PL. Analysis of Pretest-Posttest Designs. Chapman & Hall/CRC; Boca Raton: 2000.

Brand A, Richter-Landsberg C, Leibfritz D. Multinuclear NMR studies on the energy metabolism of glial and neuronal cells. Dev Neurosci. 1993; 15:289–298. [PubMed: 7805581]

Chen SQ, Cai Q, Shen YY, Wang PJ, Teng GJ, Zhang W, Zang FC. Age-related changes in brain metabolites and cognitive function in APP/PS1 transgenic mice. Behav Brain Res. 2012; 235:1–6. [PubMed: 22828014]

Chen SQ, Wang PJ, Ten GJ, Zhan W, Li MH, Zang FC. Role of Myo-Inositol by Magnetic Resonance Spectroscopy in Early Diagnosis of Alzheimer's Disease in APP/PS1 Transgenic Mice. Dement Geriatr Cogn. 2009; 28:558–566.

Choi JK, Dedeoglu A, Jenkins BG. Application of MRS to mouse models of neurodegenerative illness. NMR Biomed. 2007; 20:216–237. [PubMed: 17451183]

Choi JK, Jenkins BG, Carreras I, Kaymakcalan S, Cormier K, Kowall NW, Dedeoglu A. Anti-inflammatory treatment in AD mice protects against neuronal pathology. Exp Neurol. 2010; 223:377–384. [PubMed: 19679126]

Dedeoglu A, Choi JK, Cormier K, Kowall NW, Jenkins BG. Magnetic resonance spectroscopic analysis of Alzheimer's disease mouse brain that express mutant human APP shows altered neurochemical profile. Brain Res. 2004; 1012:60–65. [PubMed: 15158161]

DeMattos RB, Bales KR, Cummins DJ, Dodart JC, Paul SM, Holtzman DM. Peripheral anti-A beta antibody alters CNS and plasma A beta clearance and decreases brain A beta burden in a mouse model of Alzheimer's disease. Proc Natl Acad Sci USA. 2001; 98:8850–8855. [PubMed: 11438712]

Forster D, Davies K, Williams S. Magnetic Resonance Spectroscopy In Vivo of Neurochemicals in a Transgenic Model of Alzheimer's Disease: A Longitudinal Study of Metabolites, Relaxation Time, and Behavioral Analysis in TASTPM and Wild-Type Mice. Magn Reson Med. 2013; 69:944–955. [PubMed: 22760762]

Fox, J. Applied Regression Analysis and Generalized Linear Models. Sage; Los Angeles: 2008.

Freeman GB, Lin JC, Pons J, Raha NM. 39-week toxicity and toxicokinetic study of ponezumab (PF-04360365) in cynomolgus monkeys with 12-week recovery period. J Alzheimers Dis. 2012; 28:531–541. [PubMed: 22045481]

Garwood M, DelaBarre L. The return of the frequency sweep: designing adiabatic pulses for contemporary NMR. J Magn Reson. 2001; 153:155–177. [PubMed: 11740891]

Garwood M, Ke Y. Symmetric pulses to induce arbitrary flip angles with compensation for RF inhomogeneity and resonance offsets. J Magn Reson. 1991; 94:511–525.

Govindaraju V, Young K, Maudsley AA. Proton NMR chemical shifts and coupling constants for brain metabolites. NMR Biomed. 2000; 13:129–153. [PubMed: 10861994]

Gruetter R. Automatic, localized in vivo adjustment of all first- and second-order shim coils. Magn Reson Med. 1993; 29:804–811. [PubMed: 8350724]

Gruetter R, Tkac I. Field mapping without reference scan using asymmetric echo-planar techniques. Magn Reson Med. 2000; 43:319–323. [PubMed: 10680699]

Hartman RE, Izumi Y, Bales KR, Paul SM, Wozniak DF, Holtzman DM. Treatment with an amyloid-beta antibody ameliorates plaque load, learning deficits, and hippocampal long-term potentiation in a mouse model of Alzheimer's disease. J Neurosci. 2005; 25:6213–6220. [PubMed: 15987951]

Hebert LE, Scherr PA, Bienias JL, Bennett DA, Evans DA. Alzheimer disease in the US population: prevalence estimates using the 2000 census. Arch Neurol. 2003; 60:1119–1122. [PubMed: 12925369]

Hennig J, Nauerth A, Friedburg H. RARE imaging: a fast imaging method for clinical MR. Magn Reson Med. 1986; 3:823–833. [PubMed: 3821461]

Henry PG, Marjanska M, Walls JD, Valette J, Gruetter R, Ugurbil K. Proton-observed carbon-edited NMR spectroscopy in strongly coupled second-order spin systems. Magn Reson Med. 2006; 55:250–257. [PubMed: 16402370]

Holcomb L, Gordon MN, McGowan E, Yu X, Benkovic S, Jantzen P, Wright K, Saad I, Mueller R, Morgan D, Sanders S, Zehr C, O'Campo K, Hardy J, Prada CM, Eckman C, Younkin S, Hsiao K, Duff K. Accelerated Alzheimer-type phenotype in transgenic mice carrying both mutant amyloid precursor protein and presenilin 1 transgenes. Nat Med. 1998; 4:97–100. [PubMed: 9427614]

Hsiao K, Chapman P, Nilsen S, Eckman C, Harigaya Y, Younkin S, Yang F, Cole G. Correlative memory deficits, Aβ elevation, and amyloid plaques in transgenic mice. Science. 1996; 274:99–102. [PubMed: 8810256]

Jack CR Jr. Garwood M, Wengenack TM, Borowski B, Curran GL, Lin J, Adriany G, Grohn OH, Grimm R, Poduslo JF. In vivo visualization of Alzheimer's amyloid plaques by magnetic resonance imaging in transgenic mice without a contrast agent. Magn Reson Med. 2004; 52:1263–1271. [PubMed: 15562496]

Jack CR Jr. Marjanska M, Wengenack TM, Reyes DA, Curran GL, Lin J, Preboske GM, Poduslo JF, Garwood M. Magnetic resonance imaging of Alzheimer's pathology in the brains of living

transgenic mice: a new tool in Alzheimer's disease research. Neuroscientist. 2007; 13:38–48. [PubMed: 17229974]

Jansen D, Zerbi V, Janssen CIF, Dederen P, Mutsaers MPC, Hafkemeijer A, Janssen AL, Nobelen CLM, Veltien A, Asten JJ, Heerschap A, Kiliaan AJ. A Longitudinal Study of Cognition, Proton MR Spectroscopy and Synaptic and Neuronal Pathology in Aging Wild-type and A beta PPswe-PS1dE9 Mice. Plos One. 2013; 8:e63643. [PubMed: 23717459]

Kantarci K, Lowe V, Przybelski SA, Senjem ML, Weigand SD, Ivnik RJ, Roberts R, Geda YE, Boeve BF, Knopman DS, Petersen RC, Jack CR Jr. Magnetic resonance spectroscopy, beta-amyloid load, and cognition in a population-based sample of cognitively normal older adults. Neurology. 2011; 77:951–958. [PubMed: 21865577]

Karlnoski RA, Rosenthal A, Alamed J, Ronan V, Gordon MN, Gottschall PE, Grimm J, Pons J, Morgan D. Deglycosylated anti-Aβ antibody dose-response effects on pathology and memory in APP transgenic mice. J Neuroimmune Pharmacol. 2008; 3:187–197. [PubMed: 18607758]

La Porte SL, Bollini SS, Lanz TA, Abdiche YN, Rusnak AS, Ho WH, Kobayashi D, Harrabi O, Pappas D, Mina EW, Milici AJ, Kawabe TT, Bales K, Lin JC, Pons J. Structural basis of C-terminal beta-amyloid peptide binding by the antibody ponezumab for the treatment of Alzheimer's disease. J Mol Biol. 2012; 421:525–536. [PubMed: 22197375]

Little, RJA.; Rubin, DB. Statistical Analysis with Missing Data. Wiley; Hoboken, N.J: 2002.

Marjanska M, Curran GL, Wengenach TM, Henry P-G, Bliss RL, Poduslo JF, Jack CRJ, Ugurbil K, Garwood M. Monitoring disease progression in transgenic mouse models of Alzheimer's disease with proton magnetic resonance spectroscopy. Proc Nat Acad of Sci USA. 2005; 102:11906–11910. [PubMed: 16091461]

Mlynarik V, Cacquevel M, Sun-Reimer L, Janssens S, Cudalbu C, Lei HX, Schneider BL, Aebischer P, Gruetter R. Proton and Phosphorus Magnetic Resonance Spectroscopy of a Mouse Model of Alzheimer's Disease. J Alzheimers Dis. 2012; 31:S87–S99. [PubMed: 22451319]

Murray, ME.; Przybelski, SA.; Lesnick, T.; Liesinger, AM.; Spychalla, A.; Gunter, JL.; Parisi, JE.; Boeve, BF.; Knopman, DS.; Petersen, RC.; Jack, CR., Jr.; Dickson, DW.; Kantarci, K. Aberrant tau and amyloid pathology underlies proton MR spectroscopic alterations in Alzheimer's disease. Alzheimer's Association International Conference; Boston. 2013.

O'Brien PC. The appropriateness of analysis of variance and multiple-comparison procedures. Biometrics. 1983; 39:787–794. [PubMed: 6652209]

Oberg J, Spenger C, Wang FH, Andersson A, Westman E, Skoglund P, Sunnemark D, Norinder U, Klason T, Wahlund LO, Lindberg M. Age related changes in brain metabolites observed by H-1 MRS in APP/PS1 mice. Neurobiol Aging. 2008; 29:1423–1433. [PubMed: 17434239]

Pfeuffer J, Tkac I, Provencher SW, Gruetter R. Toward an in vivo neurochemical profile: quantification of 18 metabolites in short-echo-time 1H NMR spectra of the rat brain. J Magn Reson. 1999; 141:104–120. [PubMed: 10527748]

Provencher SW. Estimation of metabolite concentrations from localized in vivo proton NMR spectra. Magn Reson Med. 1993; 30:672–679. [PubMed: 8139448]

Provencher SW. Automatic quantitation of localized in vivo 1H spectra with LCModel. NMR Biomed. 2001; 14:260–264. [PubMed: 11410943]

Selkoe DJ. Deciphering Alzheimer's disease: molecular genetics and cell biology yield major clues. J NIH Research. 1995; 7:57–64.

Selkoe, DJ. Molecular pathology of Alzheimer's disease: the role of amyloid. In: Growden, editor. The Dementias: Blue Book of Neurology Series. Vol. vol. 19. Butterworth-Heinemann; Newton, MA: 1998. p. 257-283.

Senn S. Change from baseline and analysis of covariance revisited. Stat Med. 2006; 25:4334–4344. [PubMed: 16921578]

Silver MS, Joseph RI, Hoult DI. Highly selective π/2 and π pulse generation. J Magn Reson. 1984; 59:347–351.

Tkac I, Starcuk Z, Choi IY, Gruetter R. In vivo 1H NMR spectroscopy of rat brain at 1 ms echo time. Magn Reson Med. 1999; 41:649–656. [PubMed: 10332839]

van Duijn S, Nabuurs RJA, van Duinen SG, Natte R, van Buchem MA, Alia A. Longitudinal Monitoring of Sex-Related in vivo Metabolic Changes in the Brain of Alzheimer's Disease

Transgenic Mouse Using Magnetic Resonance Spectroscopy. J Alzheimers Dis. 2013; 34:1051–1059. [PubMed: 23321522]

von Kienlin M, Kunnecke B, Metzger F, Steiner G, Richards JG, Ozmen L, Jacobsen H, Loetscher H. Altered metabolic profile in the frontal cortex of PS2APP transgenic mice, monitored throughout their life span. Neurobiol Dis. 2005; 18:32–39. [PubMed: 15649694]

Westman E, Spenger C, Oberg J, Reyer H, Pahnke J, Wahlund LO. In vivo 1H-magnetic resonance spectroscopy can detect metabolic changes in APP/PS1 mice after donepezil treatment. BMC Neurosci. 2009:10. [PubMed: 19208233]

Wilcock D, Rojiani A, Rosenthal A, Levkowitz G, Subbarao S, Alamed J, Wilson D, Wilson N, Freeman MJ, Gordon MN, Morgan D. Passive amyloid immunotherapy clears amyloid and transiently activates microglia in a transgenic mouse model of amyloid deposition. J Neurosci. 2004a; 24:6144–6151. [PubMed: 15240806]

Wilcock D, Rojiani A, Rosenthal A, Subbarao S, Freeman MJ, Gordon MN, Morgan D. Passive immunotherapy against Abeta in ages APP-transgenic mice reverses cognitive deficits and depletes parenchymal amyloid deposits in spite of increased vascular amyloid and microhemorrhage. J Neuroinflamm. 2004b; 1:24.

Wilcock DM, Alamed J, Gottschall PE, Grimm J, Rosenthal A, Pons J, Ronan V, Symmonds K, Gordon MN, Morgan D. Deglycosylated anti-amyloid-β antibodies eliminate cognitive deficits and reduce parenchymal amyloid with minimal vascular consequences in aged amyloid precursor protein transgenic mice. J Neurosci. 2006; 26:5340–5346. [PubMed: 16707786]

- Evaluation of MRS as an outcome measure for detecting disease modification.
- Passive immunization in transgenic mouse model of Alzheimer's disease.
- Treatment effect detected by MRS with myo-inositol reduction.
- MRS shown to be a valid in vivo measure of anti-Aβ therapeutic efficacy.

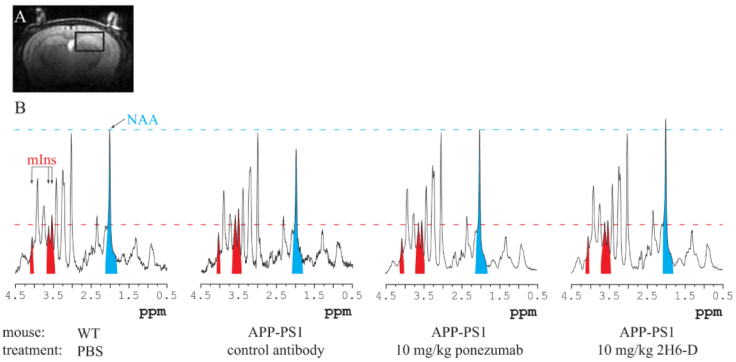

Figure 1.

(a) Representative image used for voxel placement and (b) representative spectra from different groups obtained after 4 month long treatment. The spectra are shown with similar linewidths and with amplitude adjusted using total creatine (tCr) peak at 3.03 ppm. The variation in the signal-to-noise ratio in these four spectra comes from the different line-broadening that was applied to make sure that the width of tCr peak is the same in each spectrum. The areas corresponding to NAA and mIns have been colored in blue and red respectively for visualization purposes. The largest mIns area is seen in the APP-PS1 mouse dosed with control antibody. In contrast, the APP-PS1 mice treated with 10 mg/kg ponezumab and 2H6-D show mIns peaks of similar magnitude to the WT mouse.

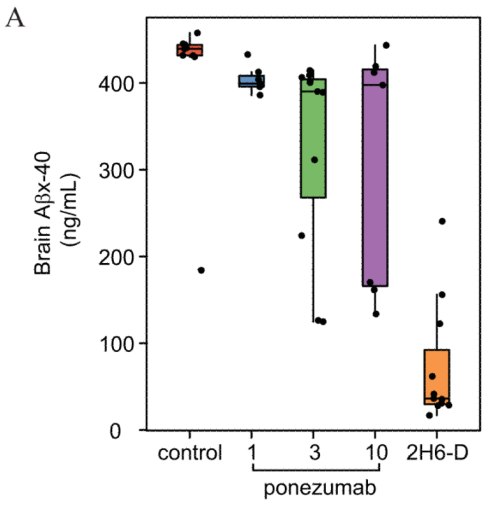

B

		control	ponezumab 1	ponezumab 3	ponezumab 10
ponezumab	1	**0.02**			
	3	**0.001**	0.29		
	10	**0.02**	0.71	0.66	
2H6-D		**<0.001**	**<0.001**	**<0.001**	**<0.001**

Figure 2.

Pairwise nonparametric Wilcoxon rank-sum/Mann-Whitney U test results for brain Aβx-40. Panel A shows box plots along with individual data points. The boxes show the 25th percentile, the 50th percentile, and the 75th percentile of the data with “whiskers” extending out 1.5 times the inter-quartile range. Panel B shows *p*-values from the pairwise comparisons.

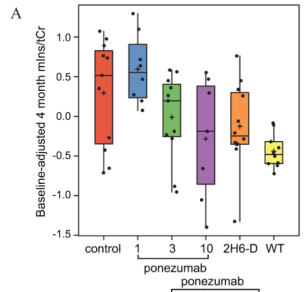

B

ponezumab	control	1	3	10	2H6-D
1	0.27				
3	0.21	**0.03**			
10	**0.04**	**0.006**	0.32		
2H6-D	**0.08**	**0.01**	0.62	0.56	
WT	**0.004**	**<0.001**	**0.08**	0.57	0.19

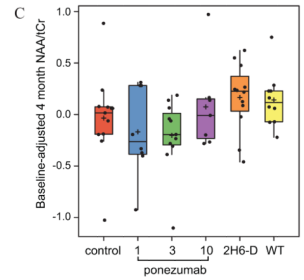

D

ponezumab	control	1	3	10	2H6-D
1	0.47				
3	0.31	0.86			
10	0.56	0.23	0.14		
2H6-D	0.22	**0.08**	**0.03**	0.62	
WT	0.32	0.14	**0.06**	0.73	0.88

Figure 3.

Analysis of covariance for (A, B) mIns/tCr and (C, D) NAA/tCr ratios. Panels A and C show box plots of partial residuals along with individual data points. The boxes show the 25th percentile, the 50th percentile, and the 75th percentile of the data with “whiskers” extending out 1.5 times the inter-quartile range. A plus sign indicates the group-wise sample mean. Panels B and D show *p*-values from the model contrasts.